

Origami constraints on the initial-conditions arrangement of dark-matter caustics and streams

Mark C. Neyrinck¹

¹*Department of Physics and Astronomy, The Johns Hopkins University, Baltimore, MD 21218, USA*

16 February 2012

ABSTRACT

In a cold-dark-matter universe, cosmological structure formation proceeds in rough analogy to origami folding. Dark matter occupies a three-dimensional ‘sheet,’ non-intersecting in six-dimensional velocity-position phase space. At early times, the sheet was flat like an origami sheet, i.e. velocities were essentially zero. The present paper further illustrates this analogy, and identifies a result of origami mathematics that applies to cosmology. We define caustics in the initial conditions (Lagrangian space) as surfaces in this sheet, along which the sheet has folded. The regions outlined by these caustics, which we call streams, may be colored according to the two possible orientations of initial basis vectors, a two-coloring such that adjacent streams are not colored the same. While this may not have clear observational consequences, it is a severe restriction on connectivity, since there are no bounds on the number of colors required to color a general arrangement of three-dimensional regions. Then, measuring the relevant quantities from N -body simulations, we explore how well outer caustics in Lagrangian space correspond to a Zel’dovich prediction, as well as to a measurement from the recent ORIGAMI algorithm.

Key words: large-scale structure of Universe – cosmology: theory

1 INTRODUCTION

On moderately large scales (not so large that it is entirely described by linear theory), the matter and galaxies in the Universe trace what is known as a cosmic web (e.g., Bond et al. 1996). Regions well under the mean density develop into voids. At higher density, the matter is arranged into planar structures known as walls or pancakes. Still higher-density matter has a filamentary morphology. At the highest densities, it is assembled into pointlike clusters, or haloes.

There are several ways to characterize these structures. Observationally, one way of identifying and defining them is by looking for depressions, ridges, and peaks in the (over)density field δ . For example, one can measure the eigenvalues of the Hessian $\partial^2\delta/\partial x_i\partial x_j$; this gives local density maxima/ridges in one, two and three dimensions (e.g., Hahn et al. 2007; Aragón-Calvo et al. 2007; Sousbie et al. 2008; Sousbie 2011). Another approach is global, defining voids to tessellate space. For instance, they can be defined as density depressions outlined by a watershed transform (Platen et al. 2007; Neyrinck 2008). In this framework, walls, filaments, and haloes are defined according to where voids meet each other, and the dimensionality of borders separating them (Aragón-Calvo et al. 2010). In cosmology, these two definitions turn out to be rather similar, but this only

is true in detail if no locally defined walls and filaments end within voids.

Another way to understand the structures is as folds in a three-dimensional manifold (‘sheet’). This is most suited to a Lagrangian viewpoint, in which mass parcels are tracked. A complementary viewpoint is called Eulerian, in which densities and velocities at fixed positions are tracked. First-order Lagrangian perturbation theory, known as the Zel’dovich (1970) approximation, already is quite useful to understand the basics of cosmological structure formation.

In this Lagrangian framework, particles in an N -body simulation can be thought of not simply as blobs of mass, but as vertices on an initially cubic grid that gravity deforms, and eventually causes to self-cross in three-dimensional position space. In six-dimensional velocity-position phase space, though, the manifold does not cross itself, a property which prompted our recent analogy to the paper-folding that occurs in origami (Falck et al. 2012). In that paper, we use an algorithm called ORIGAMI (Order-ReversIng Gravity, Apprehended Mangling Indices) to identify structures in an N -body simulation according to the number of axes along which the initial-conditions (Lagrangian) lattice has crossed itself. A couple of other recent papers have also explored the power of comparing initial to final conditions explicitly (Shandarin et al. 2011; Abel et al. 2011), for the purposes

of finding shell-crossings, and measuring the density within the phase-space sheet.

Another major application of a Lagrangian framework is the study of caustics, largely the subject of present work. A ‘caustic’ is the edge of a fold of the sheet in six-dimensional phase space. A strong observational motivation for studying caustics is that dark matter, if it annihilates, may do so most often in them, since formally the density goes arbitrarily high there. Thus they may greatly enhance observable signals from dark matter (e.g., Hogan 2001; Natarajan & Sikivie 2008; Vogelsberger & White 2011). The behavior of caustics in Eulerian space has been extensively studied. For example, catastrophe theory allows a rigorous description and classification of the kinds of caustics and structures that can develop in Eulerian space when the manifold folds and crosses itself (e.g., Arnold et al. 1982; Arnold 2001).

A Lagrangian view of the cosmic web is difficult to apply directly to observed data; however, perhaps methods that construct initial conditions from observed data could in principle allow an avenue to do so (e.g. Mohayaee et al. 2006; Lavaux et al. 2008). And, for example, tracking caustics in simulations is relevant to the caustic method of estimating galaxy-cluster masses, which uses the outer caustics of cluster haloes as observed in redshift space (Diaferio & Geller 1997).

This paper is organized as follows. In Section 2, we very briefly review some properties of origami mathematics that are applicable in cosmology. In Section 3, we apply these properties to cosmology, giving Lagrangian definitions of the concepts of ‘caustics’ and ‘streams,’ and show some relevant measurements from N -body simulations.

2 ORIGAMI MATHEMATICS

Considering how ancient the art of origami is, the mathematics of it have developed relatively recently. A relatively early result (dating to 1893) is that paper-folding is a more powerful mechanism for solving geometric and algebraic problems than the classical ruler and compass. For example, in principle it can be used to trisect an angle, and to solve some types of cubic equations (Row 1966; Martin 1998; Hull 2006). Then, in the last few decades, significant advances were made in algorithmic origami design (e.g., Lang 2003).

Here we focus on some results in ‘flat origami’ that are particularly relevant to large-scale structure. In flat origami, folding of a two-dimensional sheet is allowed in three dimensions, but the result is restricted to lie flat in a plane, i.e. it could be squashed between pages in a book without acquiring any new creases. The class of flat-foldable origami is quite large, for example encompassing the famous paper crane, similar to the model shown in Fig. 1.

There are several theorems that have been proven about flat origami (e.g., Hull 1994, 2002). The main flat-origami result that we exploit in the present paper is the two-colorability of polygons outlined by origami crease lines. That is, two colors suffice to color them so that no adjacent polygons share the same color. Here ‘adjacent’ means sharing a crease line (not just a vertex).

To see why two colors suffice, consider the paper crane shown in Fig. 1. Both sides of it are shown, along with its appearance when unfolded. Each polygon is colored white or

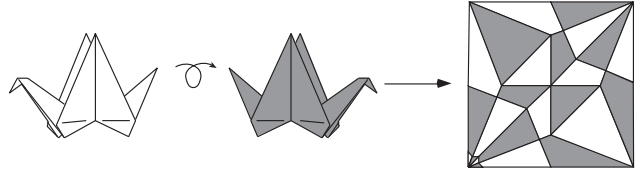


Figure 1. Two-coloring of the polygons outlined by creases in an origami ‘traditional Japanese flapping bird’ (similar to a crane). Polygons facing ‘up’ (out of the page in the leftmost diagram, with the head facing to the left) are colored white, while polygons facing ‘down’ (into the page in the leftmost diagram) are painted gray. The crane has been unfolded for the rightmost diagram. Creases are shown as lines here; the polygons outlined by them are successfully two-colored. Figure from Hull (2006), courtesy Tom Hull.

gray according to whether the polygon is facing ‘up,’ i.e. with the same orientation as it did initially, or ‘down,’ if it has been flipped over. This uniquely colors each polygon, and each crease does indeed divide ‘up’ from ‘down’ polygons.

A work of flat origami can be thought of as a function (a continuous piecewise isometry) mapping the unit square (the unfolded sheet at right in Fig. 1) into the plane. Each crease produces a reflection, reversing the direction of the vector on the paper perpendicular to the crease. The function is defined on each polygon by a sequence of these reflections. The color in each polygon corresponds to its parity, i.e. depending on whether the number of reflections used to define the function on that polygon is odd or even. It can also be measured locally with the determinant of the matrix defining the function on the polygon; we will also use this latter definition in the cosmological case below.

Besides two-colorability, there are other properties that flat-foldable crease patterns have. For example, Maekawa’s theorem states that in a flat-foldable crease pattern, the numbers of ‘mountain’ and ‘valley’ creases around a vertex differ by two. (A mountain crease becomes folded to form an upward-pointing ridge; a valley crease is folded in the opposite way.) There is not an obvious (to the author) extension of this result to cosmology, but one may exist. Another result for flat paper origami, Maekawa’s theorem, implies two-colorability through graph-theory considerations (Hull 1994). A more difficult property to test is that an arbitrary crease-pattern is physically flat-foldable without the paper intersecting any folds; this is an NP-complete problem (Bern & Hayes 1996). There are further results that, for instance, describe the angles around vertices, but they depend on the non-stretchability of the origami sheet, making them inapplicable to the cosmological case.

Fig. 2 shows a work of flat origami that bears some resemblance to a network of filaments and clusters in cosmology. Its ‘voids’ are Voronoi cells generated from the black points. Voronoi models of large-scale structure are good heuristic models of cosmological structure formation (e.g., Icke & van de Weygaert 1987; Kofman et al. 1990). The present figure corresponds most closely to a Zel’dovich-approximation evolution of particle displacements, in which structures fold up when expanding voids collide, but overshoot and do not undergo realistic further collapse. Many origami tessellations are described, with instructions, by Gjerde (2008).

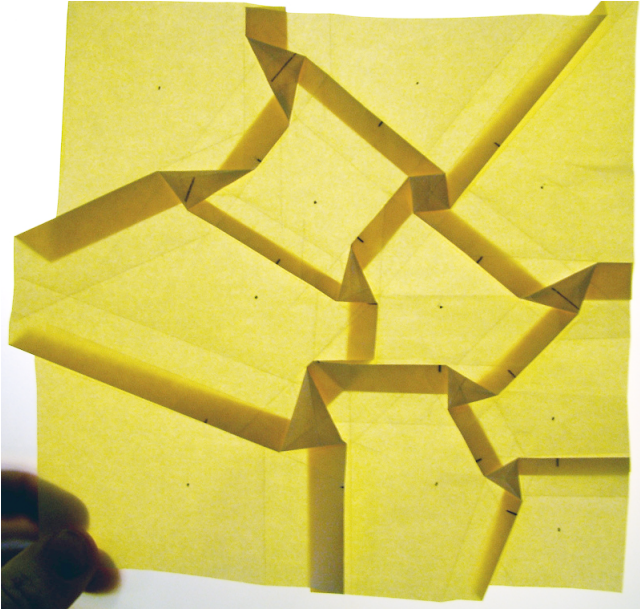


Figure 2. A Voronoi origami tessellation that bears some resemblance to cosmological voids, filaments and haloes. If the work were unfolded, the polygons outlined by creases would be two-colorable according to which way the polygon is facing. E.g. ‘voids’ and the topmost polygons in ‘haloes’ could be colored red, and the paper turned upside down within the ‘filaments’ could be colored green. The simple structure of ‘filaments’ and ‘haloes’ is as in the Zel’dovich approximation; the true universe has more complicated folding patterns, shown in subsequent figures. Figure by Eric Gjerde (<http://www.origamitessellations.com/>), used with permission.

3 APPLICATION TO COSMOLOGICAL STRUCTURES

Moving from paper origami to cosmological structure formation introduces a few changes. The manifold (sheet) has three instead of two dimensions. It folds in six dimensions (three position, and three velocity) instead of three. The sheet also stretches inhomogeneously. Moreover, the metric in six dimensions is not necessarily well-defined, although one might impose a global metric by e.g. converting velocities to positions with the Hubble constant.

In spite of these difficulties, the local parity of a patch in Lagrangian space (the initial conditions) is still easily defined, in the same way as in flat origami. Define a first-order approximation of the mapping of mass elements (particles) from initial to final coordinates as a linear transformation (called the deformation tensor) plus a translation. If the spatial resolution in Lagrangian space (i.e. the mass resolution in a simulation) is sufficiently large compared to the scale on which Lagrangian space is folding, this linear transformation is meaningful. However, deep within a halo, the spatial relationships between Lagrangian neighbors in a practical N -body simulation may become essentially random, and this condition may not be satisfied.

We may use the determinant $J(\mathbf{q})$ of this deformation tensor to measure the parity (e.g., White & Vogelsberger 2009); as mentioned above, this definition can be used in two-dimensional flat origami, as well. For example, Vogels-

berger & White (2011) use this parity measure to explore the roccoco fine-scale structure of caustics in Eulerian space.

$J(\mathbf{q})$ gives the volume of a mass element that gets deformed by the tensor, times the parity. The elements of the deformation tensor are the components of initial-conditions basis vectors transformed to the final conditions,

$$J(\mathbf{q}) = \det \left(\delta_{ij} + \frac{\partial \Psi_i}{\partial q_j} \right). \quad (1)$$

Here Ψ is the displacement field. For a mass element with Lagrangian position \mathbf{q} and Eulerian position \mathbf{x} , Ψ is defined by $\mathbf{x}(\mathbf{q}) = \mathbf{q} + \Psi(\mathbf{q})$. As usual in cosmology, we use comoving coordinates.

3.1 Streams and caustics in Lagrangian space

Caustics and streams are usually considered in Eulerian space. A caustic is a fold in projected phase space where the density formally goes infinite if particle discreteness is ignored, and the density is smoothed on arbitrarily fine scales. As for streams, at a given Eulerian-space location \mathbf{x} , there may be many of them; each stream corresponds to a point in Lagrangian space that has ended up at \mathbf{x} .

In Lagrangian space, by analogy to an unfolded origami sheet, we define a stream as a contiguous three-dimensional region with the same parity. We define a caustic as a two-dimensional surface separating streams from each other. Defined this way, a caustic indeed corresponds to a fold, since the parity swaps if one moves across it.

By definition, then, space is tessellated by streams that are outlined by caustics. The streams are also two-colorable, since the parity may take only two values.

Two-colorability may seem hopelessly academic, and indeed it does not have obvious observational consequences. But in fact it greatly restricts the arrangement of streams in three-dimensional Lagrangian space. A tessellation in greater than two dimensions has in principle no bound on its chromatic number (the number of colors required). For instance, in relation to the famous four-color theorem (four colors suffice to color any planar arrangement of regions), Guthrie (1880) discussed the difficulty of such a result in three dimensions. He imagined a set of arbitrarily many sticks, each of which touches all others. It is not hard to imagine such an arrangement, especially if the sticks are allowed to flex. In this case, the chromatic number is bounded only by the number of sticks.

In graph theory, a two-colorable graph is called bipartite (e.g., Chartrand & Zhang 2009). The vertices of our bipartite graph are the three-dimensional stream regions, and the edges (linking vertices) are the caustic surfaces between them. A bipartite graph has many properties; in fact, at least one whole book is devoted to the subject (Asratian et al. 1998). For instance, there is no path that starts and ends at the same stream region that consists of an odd number of steps from stream to stream. Considering the dual graph, in which streams and caustics swap roles, König’s theorem states that the minimum number of colors necessary for a successful coloring of caustic surfaces equals the maximum number of caustic surfaces around a single stream region.

Before continuing on to measurements from simula-

tions, we examine our definitions of streams and caustics a bit further, and problems that may arise from them.

A physical problem with our parity definition arises from a type of folding that is, in principle, possible in cosmology, but not in paper origami because the paper cannot stretch. Cosmological caustics may form in spherical or cylindrical collapse, not just planar collapse. Like planar collapse, spherical collapse reverses parity, but cylindrical collapse does not; it simply produces a 180° rotation in the two axes perpendicular to the cylinder.

However, in a physically realistic situation, the probability that more than one axis will collapse exactly simultaneously is zero. In the Zel'dovich approximation, for example, the deformation tensor will never have two exactly equal eigenvalues.

In a practical N -body simulation, the finite temporal and mass resolution will enable two- (and three-) axis crossings to happen between timesteps. In applying our parity definition to a simulation, we unfortunately miss some such unresolved caustics.

Another difficulty springs from numerical errors and errors (e.g. two-body effects) due to particle discreteness in a practical simulation. After many dynamical times suffering deep within a halo, Lagrangian mass elements may be hopelessly tangled for these reasons, and not just because of the doubtlessly plentiful caustics that have formed. Indeed, as shown in the figures below, halo regions have fairly random parities, and it is not clear whether these parities arise from physical caustics, or this numerical ‘noise.’

It may be difficult to visualize how a newly forming caustic forming in an already high-density region (already with many overlapping streams) behaves in Lagrangian space. In Lagrangian space, the caustic surface slices the various streams at various angles depending on how each stream has been rotated, stretched and reflected. But by definition, the new streams are still three-dimensional regions, divided by two-dimensional caustics.

3.2 Simulation measurements

Fig. 3 shows the folding up of a cosmological sheet of 256^2 particles from a 256^3 -particle gravitational simulation run to the present epoch. Pixels (in Lagrangian coordinates) and particles (in Eulerian coordinates) are colored according to their ORIGAMI morphologies (left) and parities (right). These colorings visually correspond quite well to where structures are after folding. There are a few regions that would look voidy if they weren't colored, but are colored nonetheless (blue at left, and orange at right). These particles have crossed others in the direction perpendicular to the page.

The upper-right panel shows a measurement from an N -body simulation of the quantity we use to determine the local parity, $J(\mathbf{q})$ from Eq. 1. This gives the volume of the mass element (inversely proportional to its density) times its parity. The parity can be read off from the color scale. Regions with right-handed parity (as in initial conditions) are black or blue; left-handed regions are white or orange. Each pixel represents a particle. In origami terms, this is the sheet before folding. Note that the magnitude is quite small in the cores of halo regions, because mass elements shrink considerably in high-density halo regions. To estimate the tensor at each

particle, we use the final-conditions separations between the six particles that initially surround the particle, i.e. $\{\mathbf{x}_{i+1,j,k} - \mathbf{x}_{i-1,j,k}, \mathbf{x}_{i,j+1,k} - \mathbf{x}_{i,j-1,k}, \mathbf{x}_{i,j,k+1} - \mathbf{x}_{i,j,k-1}\}$, where the indices refer to positions on the Lagrangian particle grid. Note that the resolution of this measurement is twice the smallest available Lagrangian length scale (the interparticle spacing).

The simulation shown was run to the present epoch using the GADGET-2 code (Springel 2005) with 256^3 particles in a box of size $64 h^{-1}$ Mpc, assuming a concordance Λ CDM set of cosmological parameters ($\Omega_b = 0.04$, $\Omega_m = 0.3$, $\Omega_\Lambda = 0.7$, $h = 0.73$, $n_s = 0.93$, $\sigma_8 = 0.81$). Before running the simulation, its initial-conditions density field was smoothed with a Gaussian of width $\sigma = 1 h^{-1}$ Mpc, inhibiting small-scale structure formation and clarifying the parity measurement. This smoothing reduced σ_8 (the dispersion in the overdensity within spheres of radius $8 h^{-1}$ Mpc) by 0.4 per cent. This small-scale power attenuation would happen in the real universe if the dark matter had substantial warmth; however, warm dark matter would also cause the three-dimensional ‘sheet’ it occupies to be smeared out by thermal motions.

There is some agreement between outer caustics identified by ORIGAMI morphology (the boundaries between black and non-black regions) and as defined by parity (the outermost boundaries between black/blue and white/orange regions), but the agreement is not perfect. There are a couple of reasons for this. First, the parity is defined on a larger grid spacing on the Lagrangian lattice (two interparticle spacings, not one). Thus, if only one particle crossed another, this would be detected by the ORIGAMI criterion but not necessarily by the parity criterion. Second, the ORIGAMI algorithm detects crossings projecting along the Eulerian (x, y, z) axes; in contrast, the parity measurement uses only the local vectors between Lagrangian neighbors. So, unlike the parity measurement, the ORIGAMI morphology is in principle sensitive to rotations (fortunately, small on cosmological scales). Still, the ORIGAMI halo, filament and wall-finder shines here, where the smoothed initial conditions produce visually obvious morphologies.

Fig. 4 is the same figure as Fig. 3, except that the simulation was run without smoothing the initial conditions. The small-scale structure in Fig. 4 makes the parity map (the upper-right panel) much more cluttered from additional structure. There are many visible extended streams (patches of identical parity), especially voids, but much of the plot looks essentially random. Halo particles (comprising most of the particles) have likely undergone many shell crossings. We again caution, however, that some of this apparent randomness could be from numerical ‘noise.’

Fig. 5 shows Lagrangian $J(\mathbf{q})$ plots, adding red contours at the Zel'dovich-approximation (Zel'dovich 1970) prediction for the position of the outermost shell crossing. In the Zel'dovich approximation, the evolution with time τ of the volume V (in units of the mean) of a mass element at Lagrangian coordinate \mathbf{q} is given by

$$V(\mathbf{q}, \tau) = \prod_{i=0}^2 [1 - \lambda_i(\mathbf{q})D(\tau)], \quad (2)$$

a product over the three eigenvalues λ_i of the deformation tensor, using the linear growth factor $D(\tau)$.

For the Zel'dovich prediction in Fig. 5, we computed

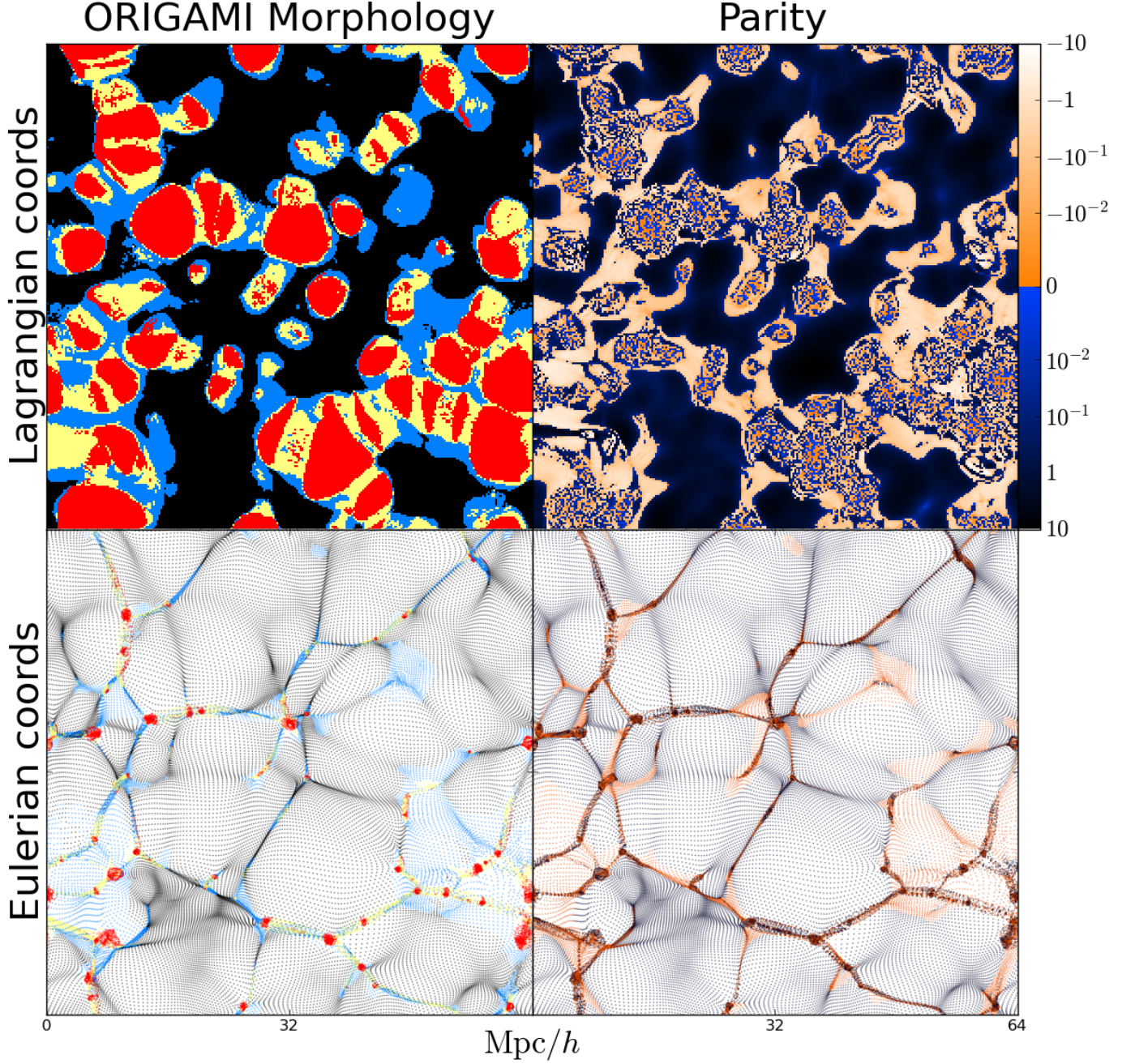


Figure 3. The folding of a cosmological sheet (top, unfolded; bottom, folded). Quantities were measured from a 256^2 sheet of particles from a 256^3 -particle Λ CDM N -body simulation; The 256^2 particles share the same z -coordinate in the initial-conditions lattice, where z points out of the page. Before running the simulation, the initial conditions were smoothed with a $1 h^{-1}$ Mpc Gaussian window, to inhibit small-scale structure formation. Top panels use Lagrangian coordinates, in which each particle is a square pixel in a 256^2 -pixel image. In the bottom panels, particles are shown in their actual present-epoch Eulerian (x, y) coordinates, projecting out the z coordinate (in which the slice does have some extent). In left-hand panels, void, wall, filament and halo ORIGAMI morphologies are shown in black, blue, yellow and red, respectively. In right-hand panels, particles are colored according to J , i.e. the volume of their fluid element times its parity. Black/blue particles have right-handed parity (as in the initial conditions), and white/orange particles have swapped, left-handed parity.

the largest eigenvalue of the deformation tensor (estimated as above) at each particle in the initial conditions at redshift $z = 75$. The red curve is the zero-contour of $[1 - \lambda_{\max} D(z = 0)]$, evolved forward to the present epoch with the ratio of growth factors $D(z = 0)/D(z = 75)$.

The agreement is rather good between the Zel'dovich prediction and actual outer-caustic locations for the smoothed simulation (left). For the unsmoothed simulation, the agreement is worse, but still not disastrous. It is not

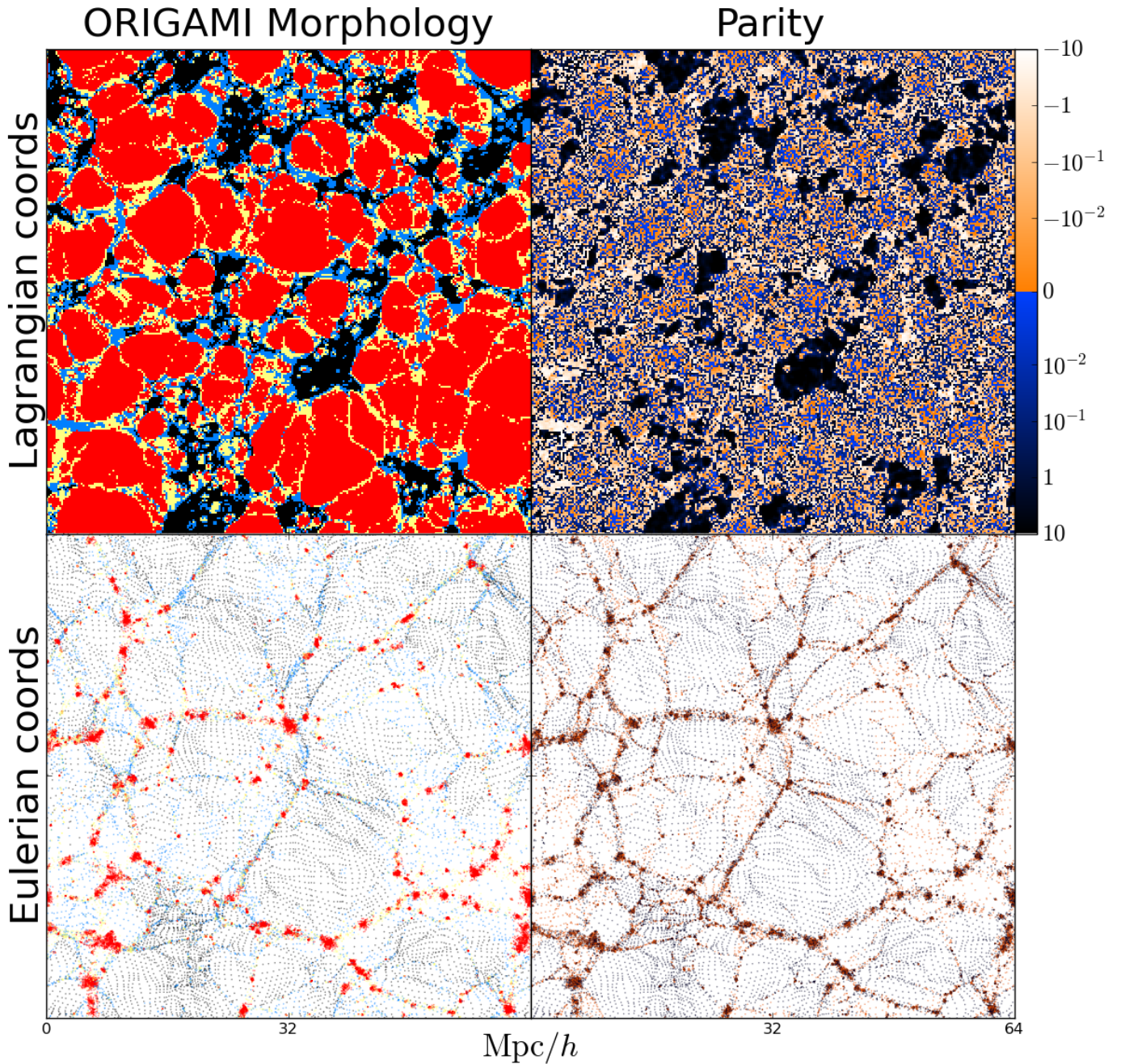


Figure 4. Same as Fig. 3, except measured from a simulation with full initial power, i.e. unsmoothed initial conditions.

surprising that the Zel’dovich approximation works best at finding large-scale caustics.

4 CONCLUSION

In this paper, we further elucidate the analogy between structure formation in cosmology and origami. We illustrate an insight from origami mathematics that appears to be applicable to cosmology: the two-colorability of three-dimensional regions (streams) outlined by two-dimensional caustic surfaces in the initial conditions. That is, two colors

suffice to color them such that adjacent regions do not have the same color, in the same way that four colors suffice to color any planar map. In fact, this result is rather trivial, if streams and caustics in Lagrangian space are defined as we do. However, a general arrangement of three-dimensional regions has no bound on the required number of colors, so this is a significant restriction on how dark matter can assemble itself into structures. Two-colorable graphs such as this have many properties that may prove useful in understanding structure formation.

While much is known about the behavior and morphology of caustics and streams in Eulerian space, their behav-

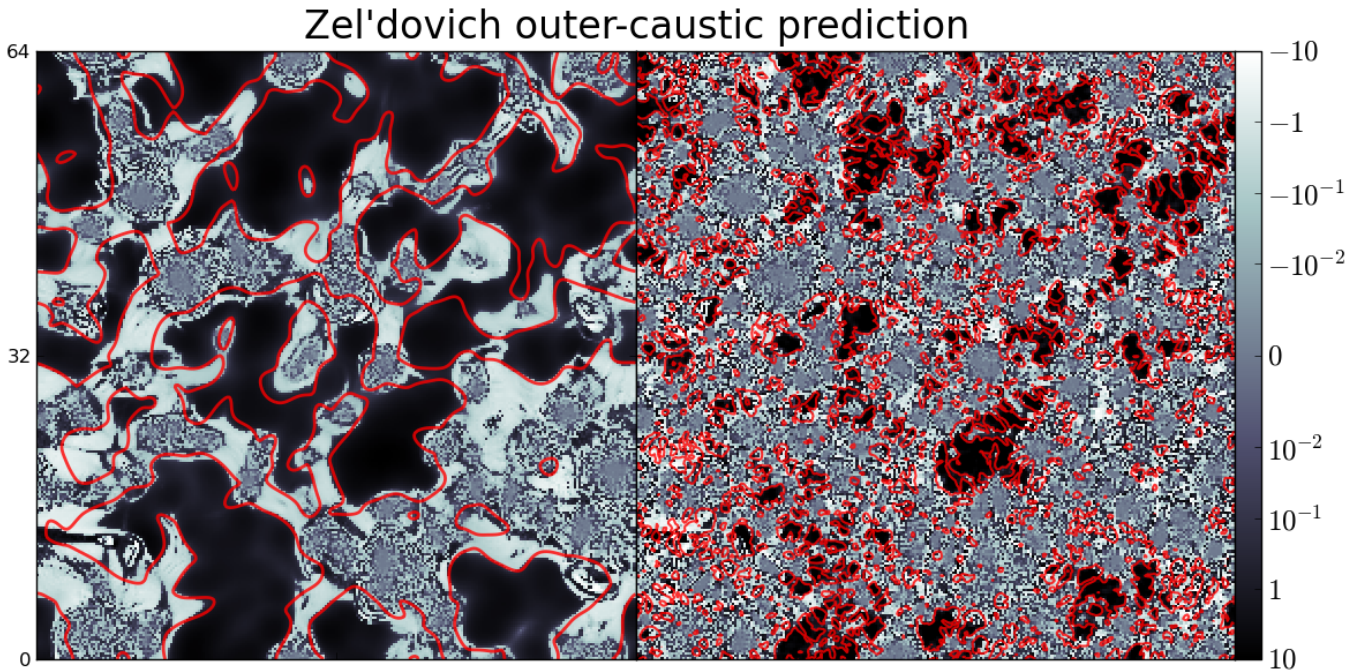


Figure 5. Comparison of a Zel’dovich prediction of where outer caustics should form (red contours) to where they actually do (boundaries between black and white regions), in the $64\text{-}h^{-1}\text{Mpc}$ simulations. In the left panel, the initial conditions have been smoothed, but not in the right panel. Pixels (corresponding to particles) are colored according to the present-epoch deformation tensor determinant $J(\mathbf{q})$. The quantities plotted under the red contours are same as in the upper-right panels of Figs. 3 and 4. However, to emphasize outer caustics, here we use a different color scale that does not particularly distinguish small negative from small positive J . The red contours show the Zel’dovich prediction, i.e. the zero-crossing of the linearly extrapolated smallest eigenvalue of the initial deformation tensor.

ior in Lagrangian space is also of interest. To our knowledge, this paper contains the first explicit illustration of the shapes of caustics and the streams in Lagrangian space. Many questions can be asked about them. How often do they meet in one-dimensional curves, and what do these one-dimensional curves represent? How often are caustic surfaces isolated?

Admittedly, two-colorability in itself is lacking in obvious observational consequences, but it is closely tied to the process of caustic formation, which is of great interest for prospective dark-matter direct and indirect detection. As cosmological simulations push to smaller and smaller scales, departing farther and farther from comfortable linear-regime physics, it is useful to know as much mathematically as possible (including the present result) about the structures that develop. It would be interesting to explore whether enforcing the properties of caustics and streams found here, or of the three-dimensional sheet structure itself, would be useful to ‘clean’ numerical noise away from simulations. The analogy to origami is likely to have pedagogical value, as well, enabling hands-on paper origami constructions of a cosmic web as in Fig. 2.

ACKNOWLEDGMENTS

I thank Miguel Aragón-Calvo for the use of the simulations presented here, and for many discussions; Robert Lang for an inspiring colloquium about paper origami, and valuable discussions; Tom Hull for permission to use Fig. 1; Eric

Gjerde for permission to use Fig. 2; Bridget Falck for interesting discussions; and Tom Bethell for many useless discussions. I am grateful for support through Alex Szalay from the Gordon and Betty Moore Foundation.

REFERENCES

- Abel, T., Hahn, O., & Kaehler, R. 2011, MNRAS, submitted, 1111.3944
- Aragón-Calvo, M. A., Jones, B. J. T., van de Weygaert, R., & van der Hulst, J. M. 2007, A&A, 474, 315, 0705.2072
- Aragón-Calvo, M. A., Platen, E., van de Weygaert, R., & Szalay, A. S. 2010, ApJ, 723, 364, 0809.5104
- Arnold, V. 2001, Singularities of Caustics and Wave Fronts, Mathematics and Its Applications (Springer)
- Arnold, V. I., Shandarin, S. F., & Zeldovich, I. B. 1982, Geophysical and Astrophysical Fluid Dynamics, 20, 111
- Asratian, A., Denley, T., & Häggkvist, R. 1998, Bipartite graphs and their applications, Cambridge tracts in mathematics (Cambridge University Press)
- Bern, M., & Hayes, B. 1996, in In Proceedings of the 7th Annual ACM-SIAM Symposium on Discrete Algorithms, 175–183
- Bond, J. R., Kofman, L., & Pogosyan, D. 1996, Nature, 380, 603, arXiv:astro-ph/9512141
- Chartrand, G., & Zhang, P. 2009, Chromatic graph theory, Discrete mathematics and its applications (Chapman & Hall/CRC)

- Diaferio, A., & Geller, M. J. 1997, *ApJ*, 481, 633, arXiv:astro-ph/9911277
- Falck, B. L., Neyrinck, M. C., & Szalay, A. S. 2012, *ApJ*, submitted, 1201.2353
- Gjerde, E. 2008, *Origami tessellations: awe-inspiring geometric designs*, Ak Peters Series (A K Peters)
- Guthrie, F. 1880, *Proc. Roy. Soc. Edinburgh*, 10, 727
- Hahn, O., Porciani, C., Carollo, C. M., & Dekel, A. 2007, *MNRAS*, 375, 489, arXiv:astro-ph/0610280
- Hogan, C. J. 2001, *Phys. Rev. D*, 64, 063515, arXiv:astro-ph/0104106
- Hull, T. 2006, *Project origami: activities for exploring mathematics*, Ak Peters Series (A.K. Peters)
- Hull, T. C. 1994, *Congressus Numerantium*, 100, 215
- Hull, T. C. 2002, in *The Proceedings of the Third International Meeting of Origami Science, Mathematics, and Education*, ed. T. C. Hull, 29
- Icke, V., & van de Weygaert, R. 1987, *A&A*, 184, 16
- Kofman, L., Pogorian, D., & Shandarin, S. 1990, *MNRAS*, 242, 200
- Lang, R. J. 2003, *Origami design secrets: mathematical methods for an ancient art*, Ak Peters Series (A.K. Peters)
- Lavaux, G., Mohayaee, R., Colombi, S., Tully, R. B., Bernardeau, F., & Silk, J. 2008, *MNRAS*, 383, 1292, 0707.3483
- Martin, G. E. 1998, *Geometric Constructions* (Springer)
- Mohayaee, R., Mathis, H., Colombi, S., & Silk, J. 2006, *MNRAS*, 365, 939, arXiv:astro-ph/0501217
- Natarajan, A., & Sikivie, P. 2008, *Phys. Rev. D*, 77, 043531, 0711.1297
- Neyrinck, M. C. 2008, *MNRAS*, 386, 2101, 0712.3049
- Platen, E., van de Weygaert, R., & Jones, B. J. T. 2007, *MNRAS*, 380, 551, 0706.2788
- Row, T. S. 1966, *Geometric Exercises in Paper Folding* (Dover)
- Shandarin, S., Habib, S., & Heitmann, K. 2011, *ArXiv e-prints*, 1111.2366
- Sousbie, T. 2011, *MNRAS*, 414, 350, 1009.4015
- Sousbie, T., Pichon, C., Colombi, S., Novikov, D., & Pogosyan, D. 2008, *MNRAS*, 383, 1655, 0707.3123
- Springel, V. 2005, *MNRAS*, 364, 1105, arXiv:astro-ph/0505010
- Vogelsberger, M., & White, S. D. M. 2011, *MNRAS*, 413, 1419, 1002.3162
- White, S. D. M., & Vogelsberger, M. 2009, *MNRAS*, 392, 281, 0809.0497
- Zel'dovich, Y. B. 1970, *A&A*, 5, 84